PERGAMON

Journal of Structural Geology 22 (2000) 1409–1425

JOURNAL OF STRUCTURAL GEOLOGY

www.elsevier.nl/locate/jstrugeo

# Closely spaced fractures in layered rocks: initiation mechanism and propagation kinematics

Taixu Bai*, David D. Pollard

*Department of Geological and Environmental Sciences, Stanford University, Stanford, CA 94305-2115, USA*

Received 15 October 1999; accepted 18 May 2000

**Abstract**

Spacings of opening-mode fractures (joints and veins) in layered sedimentary rocks often scale with the layer thickness. Field observations reveal that the ratio of fracture spacing to the thickness of the fractured layer, $S/T_f$, ranges from less than 0.1 to greater than 10. There is a critical spacing to layer thickness ratio that defines the condition of *fracture saturation*, and explains the observed spacing ratios between 0.8 and 1.2. Values of $S/T_f > 1.2$ are explained as the results of the fracturing process having not reached the saturation level. To explain ratios of $S/T_f < 0.8$, we study the possibility for *further fracture infilling*, by considering flaw distributions between adjacent fractures loaded by extension of the layer. Results show that infilling fractures grow more easily from flaws located near the interface than from those in the middle of the fractured layer. The propagation of a flaw located in the middle of the fractured layer is unstable, but for the flaw to propagate toward the interfaces, its height has to be greater than a critical size. This critical size decreases with increasing $S/T_f$. The propagation behavior of a flaw with one of its tips at the interface depends on $S/T_f$. The propagation is unstable when $S/T_f$ is greater than a critical value. When $S/T_f$ is less than this critical value, the propagation is first unstable, then stable, and then unstable again. An infilling fracture can cut through the fractured layer only if $S/T_f$ is greater than another critical value, otherwise the infilling fracture can only partially cut the fractured layer. For models with the same elastic constants for the fractured layer and the neighboring layers, this critical value is 0.546, and the minimum spacing to layer thickness ratio of fractures formed by the in filling process under extension is 0.273. © 2000 Elsevier Science Ltd. All rights reserved.

## 1. Introduction

Opening-mode fractures (joints and veins) in layered sedimentary rocks often are orthogonal to, and confined by layer boundaries (Kulander et al., 1979; Helgeson and Aydin, 1991; Gross and Engelder, 1995). These boundaries may or may not correspond to the surfaces of a single bed, but the vertical dimensions of the fractures are equal to the thickness of a mechanical layer, called the *fractured layer* (Pollard and Segall, 1987). Many field observations reveal that joint spacing in layered sedimentary rocks is proportional to the thickness of the fractured layer with the ratio of spacing to layer thickness ranging from less than 0.1 to greater than 10 (Price, 1966; McQuillan, 1973; Ladeira and Price, 1981; Narr and Lerche, 1984; Huang and Angelier, 1989; Narr and Suppe, 1991; Gross, 1993; Gross et al., 1995; Wu and Pollard, 1995; Becker and Gross, 1996).

Using a three-layer elastic model with a fractured central layer, Bai and Pollard (2000) investigated the stress distribution between two adjacent opening-mode fractures as a function of the fracture spacing to layer thickness ratio. The results show that there is a *critical spacing to layer thickness ratio*: when the fracture spacing to layer thickness ratio changes from greater than to less than the critical value (approximately 1.0) the normal stress acting perpendicular to the fractures changes from tensile to compressive. This *stress state transition* precludes further infilling of fractures unless they are driven by mechanisms other than a pure

* Corresponding author. Fax: +1 650 725 0979.
*E-mail address:* bai@pangea.stanford.edu (T. Bai).

0191-8141/00/$ - see front matter © 2000 Elsevier Science Ltd. All rights reserved.
PII: S0191-8141(00)00062-6

extension, or there are flaws that significantly perturb the local stress field between the fractures. Thus, the critical fracture spacing to layer thickness ratio defines a lower limit for fractures driven by extension in a material without significant flaws, and this also defines the condition of *fracture saturation* (Wu and Pollard, 1995).

The critical value of the fracture spacing to layer thickness ratio is independent of the remote strain of the fractured layer, but is weakly dependent upon elastic moduli and overburden stress (Bai and Pollard, 2000). With representative variation of the elastic constants of the fractured layer and the neighboring layers, and overburden stress, the critical fracture spacing to layer thickness ratio varies between 0.8 and 1.2. This covers the most commonly cited values of

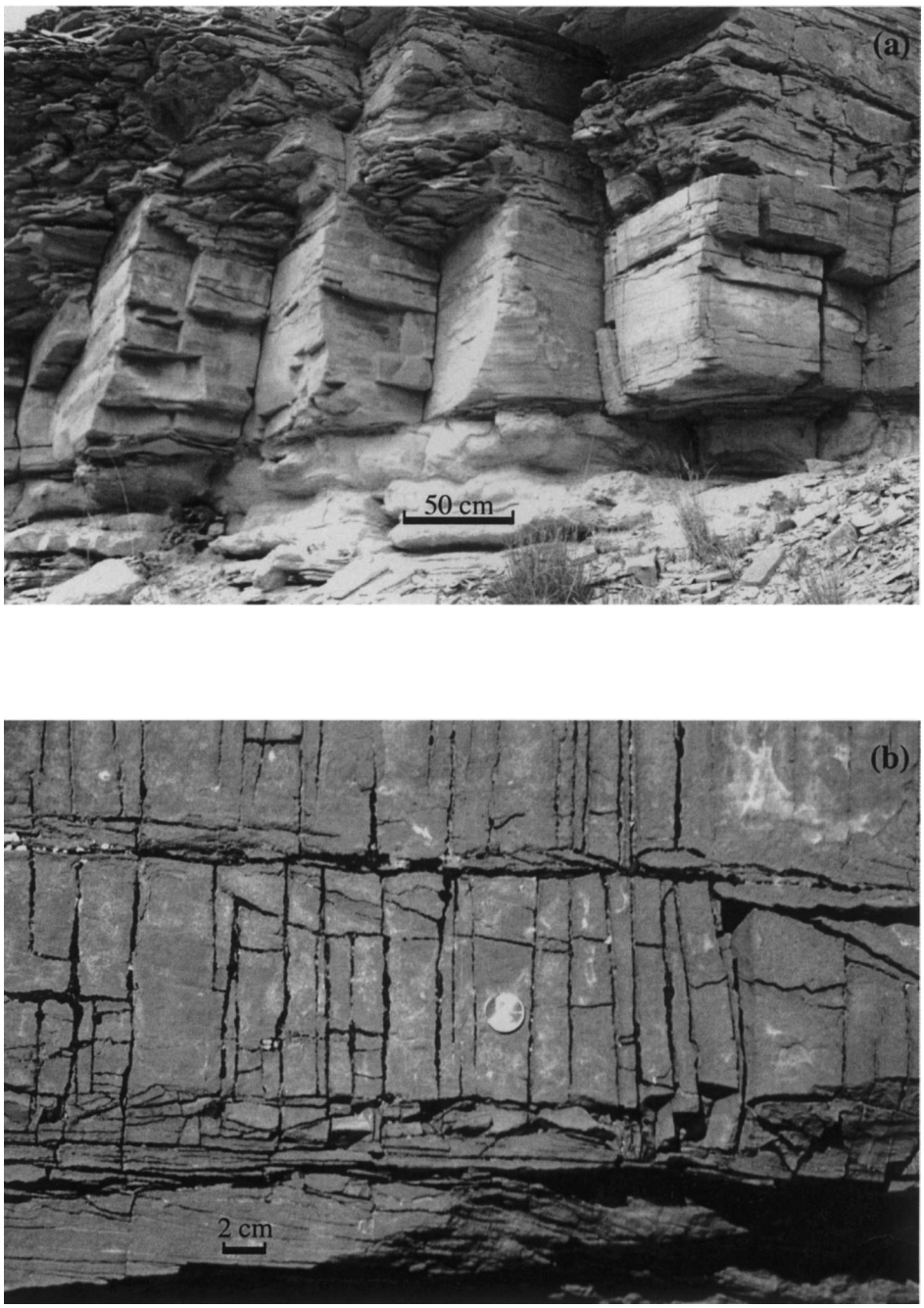


Fig. 1. Joints observed in the limestone layers of the Carmel Formation, Chimney Rock, Utah. (a) Two orthogonal joint sets usually control the outcrop pattern where the limestone layers of the Carmel Formation appear on slopes. The two joint sets are nearly orthogonal and have the same mean spacing. The mean spacing to layer thickness ratios are 0.83 based on 127 measurements. These ratios are within the range of critical spacing to layer thickness ratio (0.8–1.2). (b) Closely spaced joints. The ratios of spacing to layer thickness of these fractures are less than the lower limit of the critical spacing to layer thickness ratio (i.e. $<0.8$).

fracture spacing to layer thickness ratios in layered rocks (Fig. 1a). Fractures with spacing to layer thickness ratios greater than the critical value have not reached the status of fracture saturation. Fractures with spacing to layer thickness ratios less than the critical value are called *closely spaced fractures* (Fig. 1b), and their formation is the focus of this paper.

To explain the formation of closely spaced fractures, Ladeira and Price (1981) and Price and Cosgrove (1990) conceptually proposed that joints in thick beds (greater than 1.5 m) are produced by hydraulic fracturing. Hydraulic fracturing occurs when the fluid pressure in a flaw (small crack) exceeds the least compressive stress by an amount necessary to raise the stress intensity at the crack tip to the fracture toughness of the rock. This condition depends on the size of the flaw. As the fracture develops, there will be a fluid pressure gradient from the lower pressure in the fracture to the ambient pressure at a certain distance from the fracture (Renshaw and Harvey, 1994). Thus, at this distance a second fracture may develop from a similarly sized flaw. We do not consider this mechanism of hydraulic fracturing further in this paper. Instead, we analyze closely spaced fractures driven by a remote extension.

One of the most thoroughly investigated mechanisms for failure of rocks in compression is axial splitting. Many of the models for axial splitting are based on the *sliding crack model* (Brace and Bombolakis, 1963; Brace, 1966; Fairhurst and Cook, 1966; Horii and Nemat-Nasser, 1985; Ashby and Hallam, 1986; Kemeny and Cook, 1987; Germanovich et al., 1996). The sliding crack model consists of an initial, planar microcrack oblique to the direction of applied compressive stress. As the loading increases, the resolved shear stress exceeds the frictional resistance along the crack, and the crack faces slide past one another, forming tensile stress concentration near the crack tips. As the loading continues, the tensile stresses increase until wing cracks emerge from the sliding crack tips. As the wing cracks propagate they turn into the axial direction of maximum compressive stress. A macro fracture parallel to the maximum compressive stress is formed either by propagation of a wing crack, or linkage of several cracks.

Other mechanisms for compression induced opening-mode fracturing include the compressive–tensile stress transition around circular or elliptical openings or other cavities (Ishido and Nishizawa, 1984; Pollard and Aydin, 1988; Dyskin, 1993; Wang and Kemeny, 1994); the stress transition around stiffer or less stiff inclusions (Pollard and Aydin, 1988; Eidelman and Reches, 1992; Bessinger and Cook, 1995); and grain contact induced tensile stress (Jaeger and Cook, 1979; Gallagher et al., 1974; Pollard and Aydin, 1988).

The formation of closely spaced fractures involves the process of fracture initiation, propagation, and termination. All the mechanisms for the formation of closely spaced fractures reviewed above only explain how such fractures might be initiated. Once the fracture has initiated, the outstanding questions are whether it will continue to propagate and where it will terminate. One way of answering these questions is to study fracture surface features. As often seen on outcrops, fracture surfaces are ornamented by several geometric features such as origins, hackles and rib marks (Pollard and Aydin, 1988). These features have been used as kinematic indicators of fracture initiation points, propagation directions and propagation fronts by many authors since Woodworth (1897), including Hodgson (1961), Kulander et al. (1979), Engelder (1987), Kulander et al. (1990), DeGraff and Aydin (1987, 1993), Helgeson and Aydin (1991), Bankwitz and Bankwitz (1995), and Weinberger (1999), among others.

In this paper, we address these questions numerically by investigating the stress intensity factor of a crack-shaped flaw (i.e. ideally thin when no stress is applied) between two adjacent fractures as a function of the applied average strain in the direction perpendicular to the fractures, the spacing of the existing fractures, the position of the flaw, and the length of the flaw, using a three-layer model with a fractured central layer. In the following sections, we first introduce the numerical results. Then we discuss the implications of the results for the study of fracture spacing in layered rock and we discuss the implications for the kinematics of infilling fracture propagation.

The term 'fracture' in this paper describes a planar discontinuity that shows predominantly opening-mode displacement and cuts through the fractured layer, i.e. it extends from one of the interfaces of the fractured layer to the other. The term 'flaw' is used for a discontinuity of the same type that is very short compared to the thickness of the fractured layer. Once a flaw propagates, it becomes a 'crack' before reaching the thickness of the fractured layer. The stress intensities for flaws and cracks are used to determine whether infilling will occur by propagation.

## 2. Numerical modeling

### 2.1. Numerical method and boundary conditions

We used a two-dimensional finite element code named FRANC (FRacture ANalysis Code) to do the numerical modeling (Fig. 2). This code was developed at Cornell University and is based on the theory of linear and non-linear elastic fracture mechanics (Wawrzynek and Ingraffea, 1987). It provides a solution to the elastic boundary-value problem as well as automatic

crack propagation, remeshing, calculation of the stress intensity factors, and prediction of crack growth directions.

The theoretical basis, accuracy and friendly user interface of FRANC have been introduced by a number of authors (e.g. Wawrzynek and Ingraffea, 1987; Linsbauer et al., 1989; Ingraffea, 1990; Bittencourt et al., 1992; Fischer et al., 1995; Bittencourt et al., 1996; Bai et al., 2000). For the purposes of stress intensity factor calculation in this paper, we use three cycles of refinement of the mesh in the crack tip area. In each cycle of refinement, the radius of the elements surrounding the crack tip is reduced by half (see Fig. 2d). Also we use the modified crack closure integral technique (MCC, Rybicki and Kanninen, 1977; Raju, 1987) to calculate the stress intensity factor.

Four fractures are introduced in the fractured central layer (Fig. 2a and b). The two fractures in the middle are used to represent any two adjacent fractures in a row composed of many members. Limiting the number of fractures to four has been shown to introduce maximum errors in stress and aperture calculations of less than 2% compared to an infinite number of fractures (Bai et al., 2000; Bai and Pollard, 2000). The height of the fractures is $T_f = 20$ cm, which is also the thickness of the fractured layer. The two neighboring layers have thicknesses of $T_n = 30$ cm. The overall thickness of the model ($T = T_f + 2T_n$) is 80 cm. The width ($W$) varies according to the spacing of fractures in the model such that the distance from the left (or right) boundary to the left-most (or right-most) fracture is at least three times of the fracture height. The coordinate system is defined with the origin located at the center of the model, the $x$-axis parallel to the interface and pointing towards the right, and the $y$-axis vertical and pointing upwards. The crack-shaped flaw is introduced parallel to the fractures. The

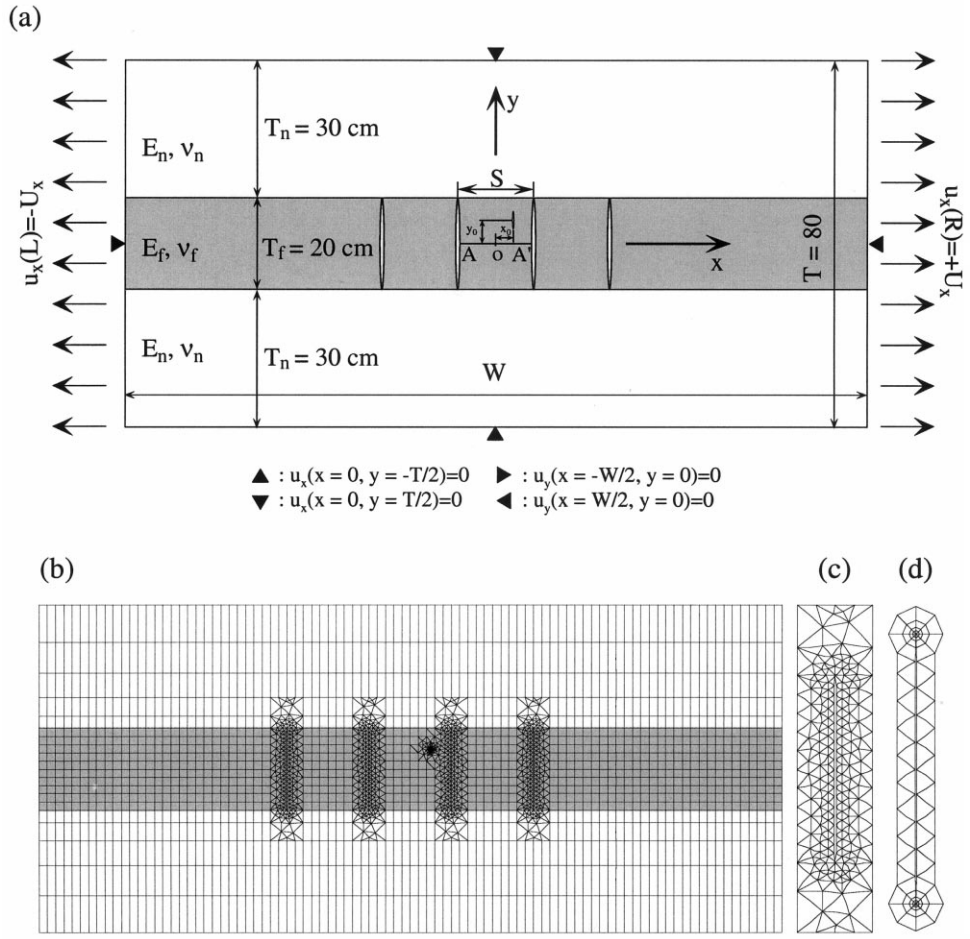


Fig. 2. (a) FEM model and its boundary conditions for layered materials with four equally spaced fractures and one flaw in the fractured layer. The variables $u_x$(L) and $u_x$(R) are the displacements imposed along the left and right boundaries, respectively. The middle points of the lower and upper boundaries are fixed in the $x$-direction. The middle points of the left and right boundaries are fixed in the $y$-directions. (b) The FEM mesh of the entire model with four fractures and one flaw. (c) Detail of the mesh around one of the fractures. (d) Detail of the mesh around the flaw. The position of the flaw is defined by the coordinates of its center. Note we use three cycles of refinement for the mesh in the flaw tip areas. In each refinement cycle, the radius of the elements surrounding the tips is reduced by half.

position of the flaw is defined by the coordinates of its center, $x_0$ and $y_0$.

The middle points of the lower and upper boundaries of the model are fixed in the $x$-direction, $u_x(x = 0, y = \pm T/2) = 0$, and the middle points of the left and right boundaries are fixed in the $y$-direction, $u_y(x = \pm W/2, y = 0) = 0$. Constant displacement conditions in the $x$-direction along the left boundary and the right boundaries are used, such that $u_x(x = \pm W/2, |y| \leq T/2) = \pm U_x$. The average strain in the $x$-direction, $\varepsilon_{xx}$(ave), is calculated as

$$\varepsilon_{xx}(\text{ave}) = 2U_x/W. \quad (1)$$

In the model, we could use contrast elastic constants for different layers. As shown by Bai and Pollard (2000), the elastic constants have only minor effects on the stress distribution between the two middle fractures. To simplify our model, we postulate the elastic materials of the fractured layer and the neighboring layers to be homogeneous and isotropic with the Young's moduli $E_f = E_n = 30$ GPa, and the Poisson's ratios $\nu_f = \nu_n = 0.25$. Also, a plane strain condition for the entire model is postulated.

### 2.2. Stress distribution between adjacent fractures without any flaw

The distributions of the normal stress in the direction perpendicular to the fractures ($\sigma_{xx}$) between the two middle fractures in the fractured layer (Fig. 2) without any flaw at different spacing to layer thickness ratios are shown in Fig. 3. The sign convention here is that tensile stress is positive and compressive stress is negative. The stress distributions are calculated for models with an average normal strain $\varepsilon_{xx}$(ave) = 0.002 across the entire model in the $x$-direction. The plots show that for fracture spacing to layer thickness ratios of 0.9 or less, there is a compressive region that extends across the central area of the model from one fracture to the other (Fig. 3a and b). In contrast, for fracture spacing to layer thickness ratios of 1.0 or greater, the compressive region is confined to the region immediately adjacent to the fractures (Fig. 3c and d). For the case with the same elastic constants for the fractured layer and the neighboring layers, the critical spacing to layer thickness ratio is 0.976 where no compressive stress is found at the central point ($x = 0$, $y = 0$) (Bai and Pollard, 2000).

The stress state transition implies that a new fracture

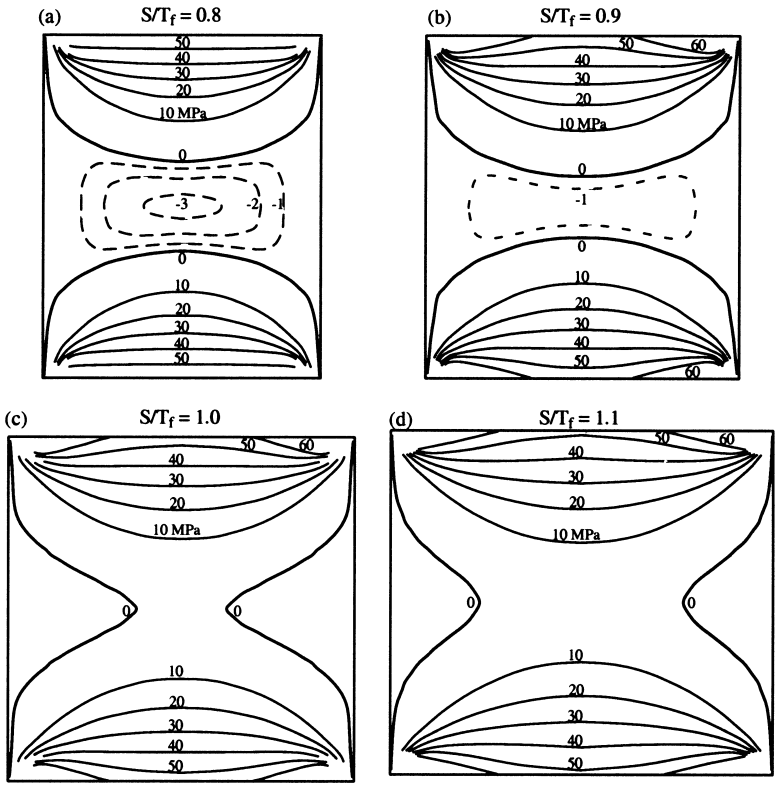


Fig. 3. Contours of the normal stress component in the direction perpendicular to the fractures ($\sigma_{xx}$) in the fractured layer between the two middle fractures at different fracture spacing to layer thickness ratios ($S/T_f$). (a) $S/T_f = 0.8$. (b) $S/T_f = 0.9$. (c) $S/T_f = 1.0$. (d) $S/T_f = 1.1$. Note that when $S/T_f$ is 0.9 or less, $\sigma_{xx}$ is compressive (dashed contours) in the central area between the two fractures; whereas when $S/T_f$ is 1.0 or greater, the stress $\sigma_{xx}$ is tensile.

cannot fill in between two fractures with a spacing to layer thickness ratio less than the critical value unless a flaw exists in the middle of the fractured layer, that cuts through the compressive region. Another possible exception is that a flaw near one of the interfaces propagates toward the other, and cuts through the region of compressive stress. Therefore, to study *further fracture infilling* between two fractures with a spacing to layer thickness ratio less than the critical value, two factors need to be considered: one is the location of the flaw; the other is the size of the flaw.

### 2.3. Stress intensity factor and flaw location

We put a flaw between the two middle fractures (see Fig. 2a and the inset of Fig. 4) with a height of $0.01T_f$. Because the finite element code (FRANC) cannot prevent material interpenetrating along the crack when the normal stress along the crack is compressive (negative), a negative stress intensity is obtained in some cases (refer to Fig. 4). Physically the negative stress intensity factor is unrealistic and should be taken as zero stress intensity (Wawrzynek and Ingraffea, 1987). The stress intensity factors at the flaw tips simply scale with the applied average strain and do not change sign (see the discussion after Eq. (2) about the negative stress intensity) as the strain is increased. For our purpose, a positive value of the stress intensity factor implies propagation, whereas a negative value implies no propagation. Thus the magnitude of the applied average strain is arbitrarily chosen as $\varepsilon_{xx}(\text{ave}) = 0.002$. The fracture spacing to layer thickness ratio for the model is 0.8, less than the critical value defined by the stress transition (i.e. 0.976), so we expect no infilling unless the flaw can propagate across the entire layer.

The stress intensity factors of the flaw are calculated for two cases. In the first case, the flaw (called the 'top' flaw) is located with its upper tip at the upper interface of the fractured layer ($y_0/T_f = 0.995$). In the second case, the flaw (called the 'middle' flaw) center is at the middle of the fractured layer ($y_0/T_f = 0$). The calculated stress intensity factors are normalized by the stress intensity factor of an internal flaw of length $T_f$ in an infinite, homogeneous, isotropic, and elastic medium with a remote loading of a unit tensile stress in the direction perpendicular to the flaw. That is

$$K_0 = (1\ \text{MPa})\sqrt{\pi T_f/2}. \tag{2}$$

The normalized stress intensity factor for the middle flaw and that for the lower tip of the top flaw are plotted vs. the horizontal position of the flaw normalized by the thickness of the fractured layer ($x_0/T_f$) in Fig. 4. Note that the stress intensity for the flaw at the middle of the fractured layer is negative. Also, the stress intensity for the middle flaw is less than that for the lower tip of the top flaw. These results imply that the middle flaw of the given size cannot propagate

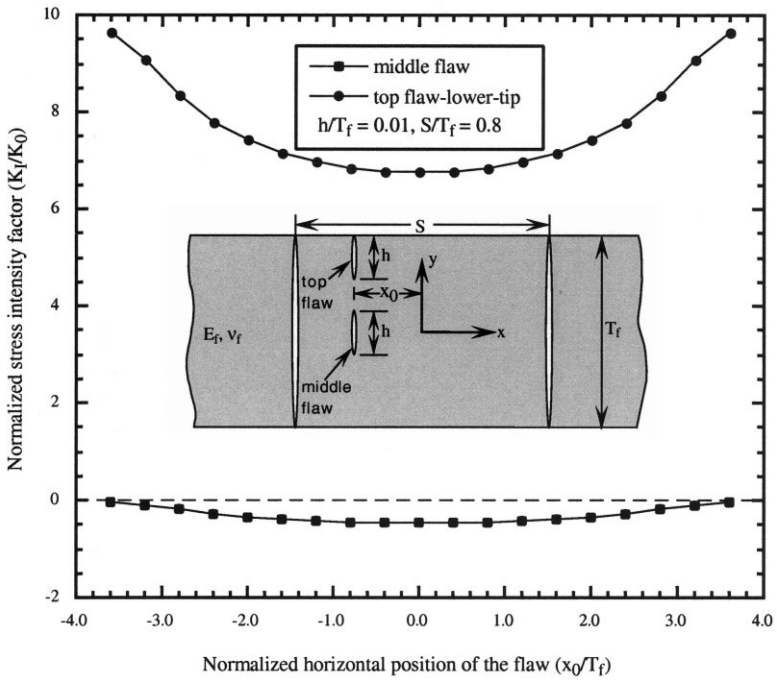


Fig. 4. Plots of the normalized stress intensity factors for the flaws located at the middle and at the top of the fractured layer, respectively, vs. the horizontal position of the flaw normalized by the thickness of the fractured layer. The plots show that the stress intensity for the lower tip of the top flaw is always positive. The stress intensity for the middle flaw is always negative.

toward the interfaces to form a complete fracture. However, the flaw at the top of the fractured layer could begin to propagate downward toward the lower interface of the fractured layer to form a complete fracture. Because of the symmetry of the problem, we also conclude that a flaw at the bottom of the fractured layer could begin to propagate toward the top.

To understand the behavior of a flaw in an arbitrary vertical location, we put a flaw of the same size (i.e. $0.01T_f$) exactly between the two middle fractures ($x_0/T_f$) and vary its vertical location. The normalized stress intensity factors for both the upper and lower tips of flaw are plotted vs. the vertical location of the flaw normalized by the thickness of the fractured layer in Fig. 5. The stress intensity factor for the tip at a greater distance from the central line of the fractured layer ($x$-axis) is systematically greater than that for the other tip. This suggests that a flaw between two fractures would tend to propagate from the tip that is further away from the central line of the fractured layer. Also, the stress intensity for both tips decreases as the flaw center approaches the central line of the fractured layer, and becomes negative when the flaw center is very close to the central line. This implies that flaws closer to the interfaces are more likely to propagate, all else being equal, and flaws of this size near the central line are unlikely to propagate.

### 2.4. Stress intensity factor and crack height (length)

The propagation of a crack between two fractures is investigated by studying the stress intensity factor of a crack located between the two middle fractures as a function of the crack height. In the first case, we calculate the stress intensity at the tips of the crack located at the center of the model (the origin of the coordinate system). In the second case, the stress intensity is calculated for the lower tip of the crack with its upper tip located at the upper interface of the fractured layer. In both cases, the applied strain is $\varepsilon_{xx}(\text{ave}) = 0.002$.

#### 2.4.1. Propagation of a crack located at the central point of the model

The normalized stress intensity at the tip of the crack is positive and increases monotonically with increasing crack height (Fig. 6) when the spacing to layer thickness ratio is greater than the critical value (i.e. 0.976, see the plot for $S/T_f = 1.0$). However, for models with a spacing to layer thickness ratio less than the critical value, the stress intensity is negative before the crack reaches a critical height. This is called *the critical crack size* ($h_c$) and is determined by

$$K_I(h_c) = 0 \tag{3}$$

where $K_I$ is the stress intensity factor of the crack. The stress intensity is positive *when the crack height is*

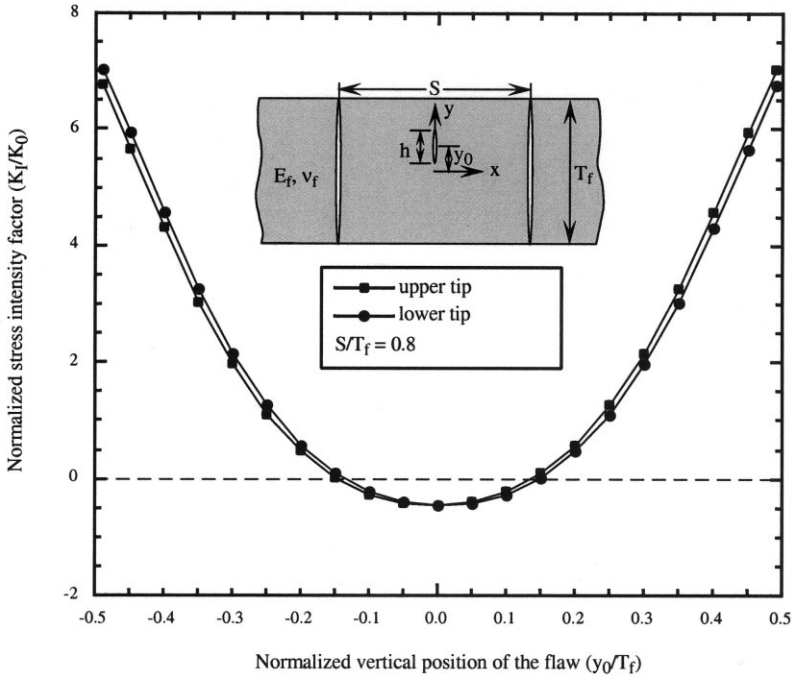


Fig. 5. Normalized stress intensity factors for a flaw located between the two middle fractures in Fig. 2(a) vs. the vertical location of the flaw, where the vertical location is normalized by the thickness of the fractured layer. The figure shows that the stress intensity factor at both tips of the flaw decreases as the flaw approaches the middle line of the fractured layer, and the stress intensity factor of the tip further away from the middle of the fractured layer is greater than that of the other tip.

*greater than the critical size*, and increases monotonically with increasing crack height. These results imply that once a crack located at the central point of the model starts to propagate, it will propagate all the way to the interfaces.

One way to characterize the behavior of crack propagation is to investigate the slope of the stress intensity factor vs. crack height plot, i.e. $dK_I/dh$ (Nemat-Nasser et al., 1980). The crack propagation is termed *stable*, when $dK_I/dh < 0$; and *unstable*, when $dK_I/dh \geq 0$. According to this criterion, the propagation of the crack from the central point is unstable when the crack height is greater than the critical size.

In order for a crack located at the central point of the model to propagate, its height has to be greater than the critical crack size (Fig. 6). The critical size decreases with increasing fracture spacing to layer thickness ratio (Fig. 7). At the critical spacing to layer thickness ratio defined by the stress state transition, the critical size reduces to zero.

### 2.4.2. Propagation of a crack with one tip located at the interface of the fractured layer

The stress intensity calculated for the lower tip of the crack with its upper tip located at the upper interface of the fractured layer is shown in Fig. 8. The sign and behavior of the stress intensity factor with increasing crack height depends on the ratio of fracture spacing to layer thickness. For large fracture spacing to layer thickness ratios (Fig. 8, the plots with $S/T_f = 1.6$ and greater), the stress intensity factors are positive and increase with increasing crack height. For intermediate fracture spacing to layer thickness ratios (Fig. 8, $S/T_f = 0.6$–$1.5$), the stress intensity factors are positive and first increase, then decrease, and then increase again, with increasing crack height.

For small fracture spacing to layer thickness ratios (Fig. 8, $S/T_f = 0.2$ and 0.4), the variation of the stress intensity factors with increasing crack height is similar to the case with intermediate fracture spacing to layer thickness ratios. However, the stress intensity factor is not always positive. In fact, it changes from positive to negative, and back to positive again, with increasing crack height. This implies that there is a *limited height for the infilling fracture* ($h_{lim}$), which is defined by

$$K_I(h_{lim}) = 0, \text{ and } \frac{d\,K_I(h_{lim})}{d\,h} < 0. \quad (4)$$

The limited infilling crack height vs. fracture spacing to layer thickness ratio is plotted in Fig. 9. The *critical fracture spacing to layer thickness ratio for complete infilling* is 0.546 for the model with the same elastic constants for the fractured layer and the neighboring layers. This value was obtained by trial and error and with the criterion that the normalized stress intensity

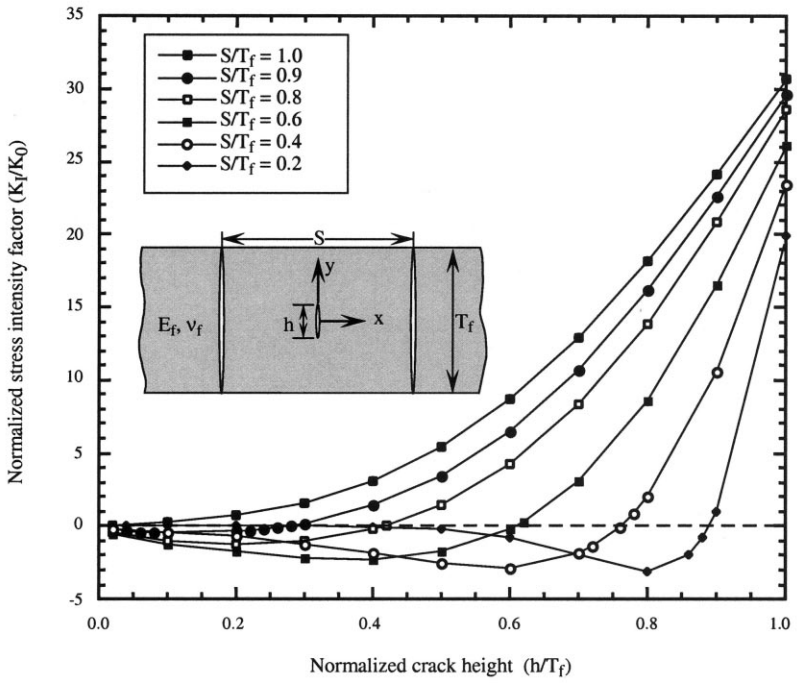


Fig. 6. Normalized stress intensity factor for a crack located at the center of the model as a function of its height (length of flaw) at different fracture spacing to layer thickness ratios. The figure shows that when the fracture spacing to layer thickness ratio is less than the critical value ($S_{cr}$) the crack has to be larger than a critical size ($h_c$) in order for it to propagate. Also, once the crack starts to propagate, it will propagate through to both of the interfaces.

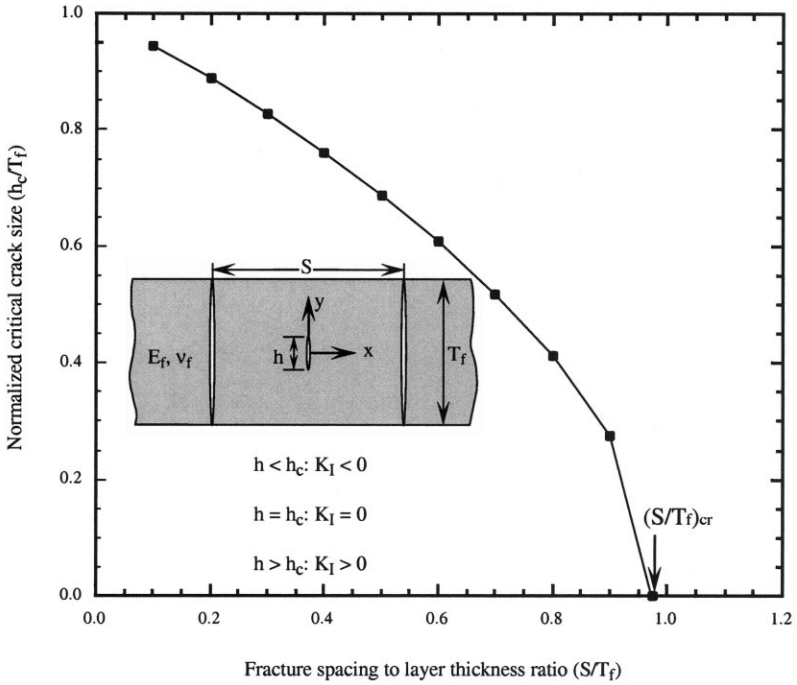


Fig. 7. The critical crack size ($h_c$) decreases with increasing fracture spacing to layer thickness ratio. At the critical spacing to layer thickness ratio ($S_{cr}$), the critical crack size ($h_c$) approaches zero.

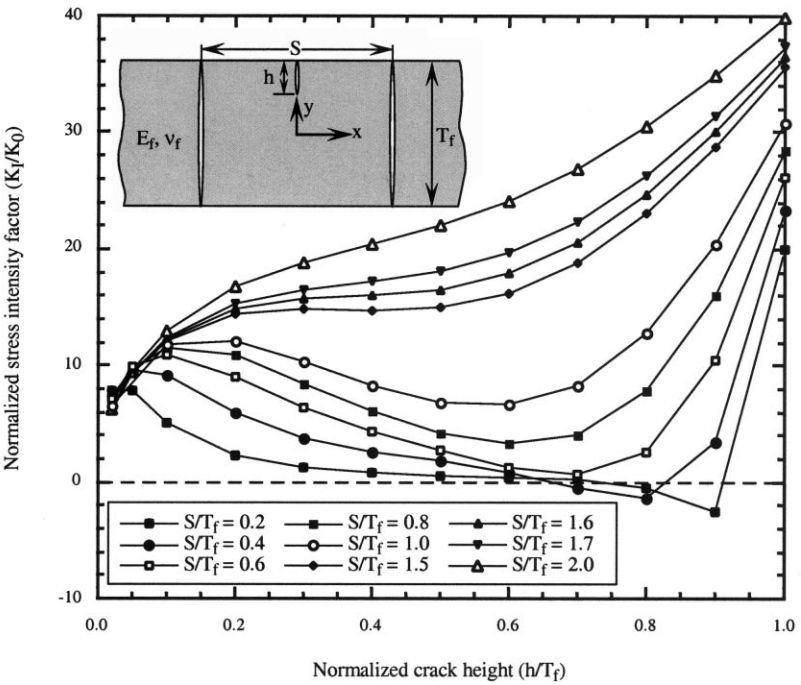


Fig. 8. Stress intensity for the lower tip of a crack with its upper tip at the upper interface of the fractured layer plotted as a function of the crack height (length of crack). Note that for large fracture spacing to layer thickness ratios (1.6, 1.7 and 2.0), the stress intensity increases with increasing crack height. For intermediate fracture spacing to layer thickness ratios (0.6–1.5), the stress intensity is always positive, and first increases, then decreases, and then increases again, with increasing crack height. For small fracture spacing to layer thickness ratios (0.2 and 0.4) the stress intensity becomes negative when the crack reaches a certain height.

at the lower tip of the crack is zero (i.e. the absolute value is less than $10^{-6}$) at only one point, and is positive along the rest of its path. Thus, when the spacing to layer thickness ratio is greater than this value, the infilling crack can cut the fractured layer from one interface to the other (Fig. 10d). Otherwise, the infilling crack can only partially cut the fractured layer (Fig. 10a–c). In other words, the smallest fracture spacing to layer thickness ratio for the model configuration in this study is 0.273.

The values of $dK_I/dh > 0$ when $S/T_f$ is 1.6 or greater, i.e. the crack propagation is unstable (Fig. 11). For $S/T_f$ values less than 1.5, the crack propagation first is unstable, then stable, and then unstable again. Using these results, we define a critical fracture spacing to layer thickness ratio, $(S/T_f)^u_{cr}$. The ratio $(S/T_f)^u_{cr}$ is defined by the criterion that the crack propagation is unstable (i.e. $dK_I/dh \geq 0$) for any $S/T_f \geq (S/T_f)^u_{cr}$. As shown in Fig. 11, the ratio $(S/T_f)^u_{cr}$ is between 1.5 and 1.6. Using the techniques of linear interpolation, we find $(S/T_f)^u_{cr} = 1.53$.

## 3. Discussion

We have shown that the concept of fracture saturation may break down given the right size and distribution of flaws in the fractured layer. In this section, we explain field measurement data of joint spacing from the literature using our numerical results. Then we discuss the relation between closely spaced fractures and strain localization. Finally, we discuss the implications of the numerical results for joint initiation, propagation and termination.

### 3.1. Explanations for joint spacing data from the literature

Bai and Pollard (2000, Table 1) classified joint spacing data from the literature into four ranges based on the spacing to layer thickness ratios. These are

Range I: $S/T_f > 1.2$;
Range II: $0.8 \leq S/T_f < 1.2$;
Range III: $0.3 \leq S/T_f < 0.8$;
Range IV: $S/T_f < 0.3$.

They explained the spacings in Range I ($S/T_f > 1.2$) as the jointing process in the beds having not reached the saturation level. The spacings in Range II ($0.8 \leq S/T_f < 1.2$) correspond to the critical spacing to layer thickness ratio defined by the stress state transition, i.e. spacing at or near the saturation level.

From our numerical modeling, we see that an infilling crack between two fractures with a spacing to layer thickness ratio greater than the critical value for complete infilling can cut through the fractured layer. However, an infilling crack between two fractures with a spacing to layer thickness ratio less than the critical value for complete infilling can only partially cut the

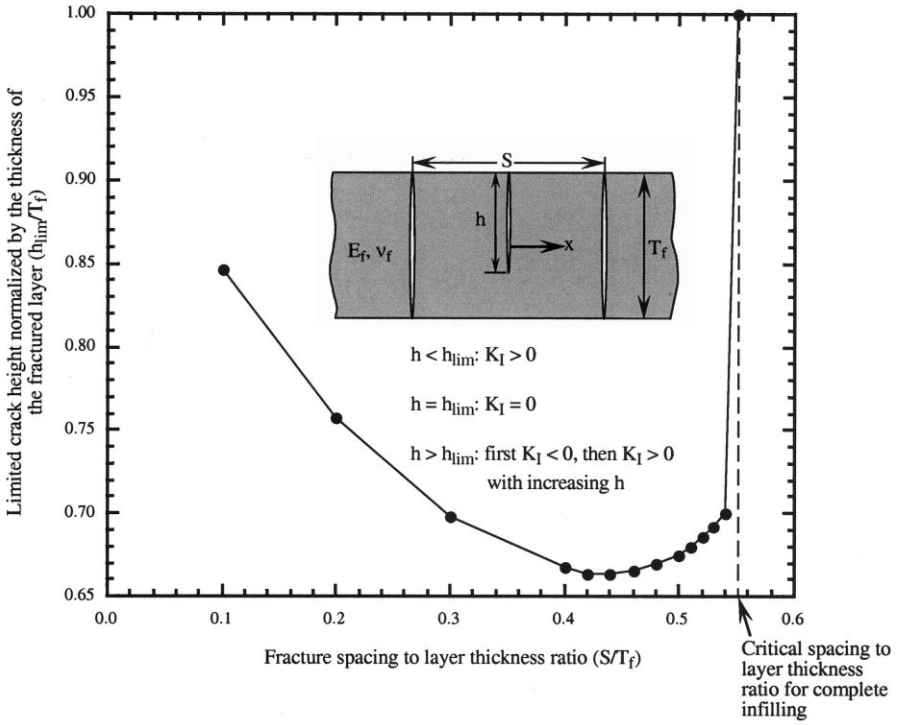


Fig. 9. The maximum limit on crack height plotted as a function of fracture spacing to layer thickness ratio.

fractured layer. The critical spacing to layer thickness ratio for complete infilling is 0.546 for the case with the same elastic constants for the fractured layer and the neighboring layers. This means that the minimum spacing to layer thickness ratio for a fracture set at complete infilling would be 0.273. As shown by Bai and Pollard (2000), the critical fracture spacing to layer thickness ratio defined by the stress state transition increases with increasing ratio of Young's modulus of the fractured layer to that of the neighboring layers, and decreases with increasing a factor based on Poisson's ratios (D, see Bai and Pollard, 2000, eq. 7). However, the effects of the elastic constants on the critical spacing to layer thickness ratio defined by the stress transition are minor (figures 4 and 5 in Bai and Pollard, 2000). We expect the same behavior for the critical fracture spacing to layer thickness ratio for complete infilling. We conclude that the spacings in Ranges III fall within the range between the critical ratio for complete infilling and the critical ratio defined by the stress state transition.

For joints with spacings in Range IV, our modeling

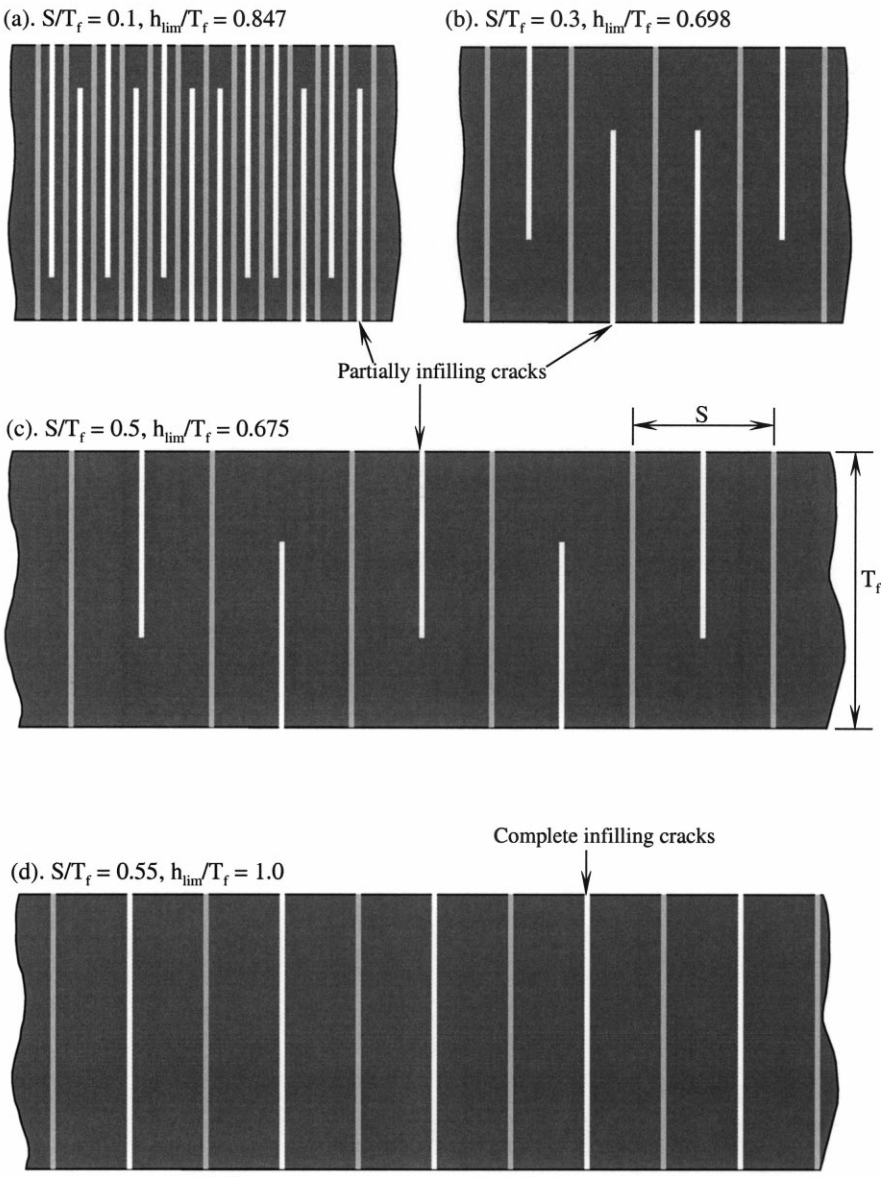


Fig. 10. (a–c) Physical views of partially infilling cracks when the fracture spacing to layer thickness ratio is less than the critical value $(S/T_f)^u_{cr}$ for complete infilling. Partially infilling occurs because the stress intensity factor of the infilling fractures changes from positive to negative as $h$ increases from less than to greater than $h_{lim}$. For a crack to grow, its calculated stress intensity factor has to be equal to or greater than the fracture toughness of the material, which is positive. For a negative stress intensity factor, it can never be equal to or greater than a positive fracture toughness. Hence, the crack has to stop when $h$ reaches $h_{lim}$. (d) Complete infilling occurs when the spacing to layer thickness ratio is greater than the critical value $(S/T_f)^u_{cr}$. This is because the stress intensity factor of the crack is always positive.

results indicate that a loading system other than extension in the direction parallel to the bedding must operate. Joint patterns, as shown in Fig. 10(a) through (c), i.e. partially infilling, are expected. One exceptional case is that a crack propagating from the upper interface downward could join another crack that propagated upward from the lower interface. In this way, a complete fracture could be formed. We think that such an exceptional case may be rare, and that it is more reasonable to seek other mechanisms for the formation of joints with spacing to layer thickness ratios in Range IV, such as natural hydraulic fracturing or axial splitting.

### 3.2. Role of average strain on the formation of closely spaced fractures

The stress intensity factor of any crack in the layered system simply scales with the applied average strain. In other words, the stress intensity at any crack tip in the layered system is linearly related to the applied average strain. In determining whether a crack will propagate, we use the criterion $K_I \geq 0$. This only implies the possibility for crack propagation. Whether the crack can propagate also depends on the relative magnitudes of the stress intensity factor and the fracture toughness of the material (Lawn, 1993; Anderson, 1995). For a given material, the greater the strain magnitude, the more likely the infilling cracks will cut through the fractured layer. This is valid for the crack infilling between two fractures with a spacing to layer thickness ratio greater than the critical ratio for complete infilling. However, if the fracture spacing to layer thickness ratio is less than the critical ratio for complete infilling, the infilling crack can only partially cut the fractured layer no matter how great the strain magnitude, because increasing the strain magnitude cannot change the sign of the stress intensity factor from negative to positive.

Becker and Gross (1996) and Gross et al. (1997) reported some very closely spaced joints with a spacing to layer thickness ratio of 0.11 from an outcrop south of Beer Sheva, Israel. They proposed that the closely spaced joints were caused by a localized high strain magnitude. Our numerical results imply that if the sequential infilling process occurred in this case, no further infilling should have occurred after the spacing to layer thickness ratio reached about 0.3. In order for the infilling joints to cut the fractured layer, mechanisms other than pure extension must have played a role during the infilling process, such as hydraulic fracturing. However, there is no evidence for abnormal fluid pressures during the formation of the closely spaced joints at Beer Sheva based on field observations (Gross, personal communication). On the other hand, even if there were high fluid pressures, it does not mean that the existence of the fluid would have been recorded in the rock record. To verify the role of fluid pressure in the formation of closely spaced joints,

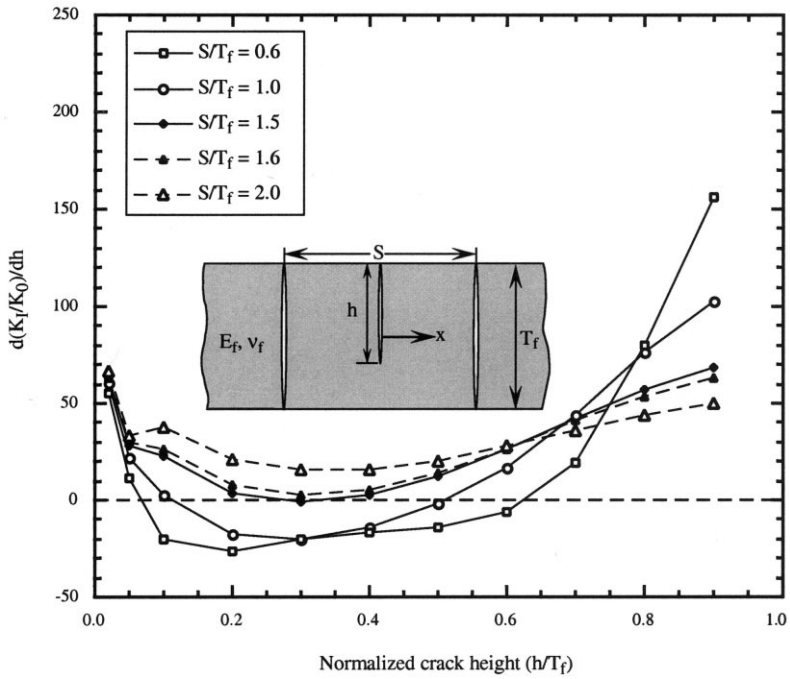


Fig. 11. Plots of $dK_I/dh$ vs. normalized crack height for models of different fracture spacing to layer thickness ratios. The figure shows that for large fracture spacing to layer thickness ratios (1.6, 1.7 and 2.0), the crack propagation is unstable, i.e. $dK_I/dh > 0$ over all values of $h$. For small fracture spacing to layer thickness ratios (0.2–1.5), the crack propagation is first unstable, then stable, and then unstable again.

more work needs to be done: both field observations and numerical modeling with pressure boundary conditions along the crack surfaces.

### 3.3. Initiation points of infilling fractures

For the model with a spacing to layer thickness ratio less than the critical value defined by the stress state transition, the stress intensity factor at the lower tip of a 'top' flaw is positive and greater than the stress intensity factor for a 'middle' flaw (Fig. 4). Also, in terms of the vertical location of the flaw, the stress intensity factor for the tip that lies at a greater distance from the central line of the fractured layer ($x$-axis) is systematically greater than that for the other tip (Fig. 5). These results imply that an infilling fracture is more likely to be initiated from a flaw located near the top or bottom of the fractured layer than from a flaw located in the middle of the fractured layer. In other words, the initiation points of infilling fractures are more likely located at or near the interfaces.

For fractures that initiate and develop before infilling, there is no obvious preference for the location of their origins based on our modeling results. However, field observations from the Genesee Group of the Appalachian Plateau, central New York, indicate that the initiation points of joints in the layered siltstone and shale turbidite are almost always located at bedding interfaces (Helgeson and Aydin, 1991; Fig. 12). It is quite likely that the joints from the Appalachian Plateau include both pre-existing joints and infilling joints. In this case, both pre-existing joints and infilling joints were initiated from the flaws at the interfaces. To further verify the implications of the modeling results, more investigations of joint surface markings need to be made using the techniques outlined by Woodworth (1897), Hodgson (1961), Kulander et al. (1979), DeGraff and Aydin (1987), and many others.

### 3.4. Propagation directions of infilling fractures

As shown in Figs. 4–6, 8 and 15, the stress intensity factor of the crack depends on its height, location, and the spacing to layer thickness ratio of the fractures. Here we assume that the crack propagation criterion is satisfied, i.e. the stress intensity factor of the crack is equal to or greater than the fracture toughness of the material, along all its way toward becoming a complete fracture, and discuss what we would expect to see on the surface of the infilling fracture.

Ideally, a crack initiated at the middle of the fractured layer will propagate upward and downward symmetrically to the interfaces and form a through fracture for the model configuration used in this study, because the stress intensity factors for the upper and lower tips of a crack located at the middle of the model are identical (Fig. 6). In this case, the origin of the infilling fracture will be at the middle line of the fractured layer, and hackles and rib marks will be symmetric about the middle line of the fractured layer (Fig. 13a).

If an infilling crack is developed from an origin located in the upper or lower half of the fractured layer, it will first propagate toward the interface closer to the initiation point, then toward the other. This is determined by the relative magnitude of the stress intensity factors for the two tips of a crack located at the origin of the fracture (Fig. 5). The hackles and rib

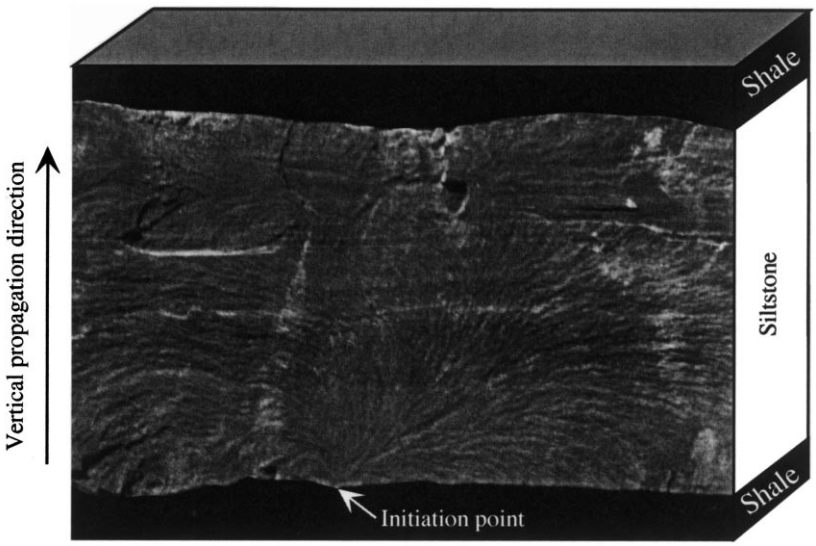


Fig. 12. Surface features of a joint in a siltstone layer from the Appalachian Plateau. As reported by Helgeson and Aydin (1991), the initiation points of joints in the siltstone and shale layers are almost always located at the interfaces. Photo provided by Atilla Aydin.

marks are not symmetric about the middle line of the fractured layer in this case (Fig. 13b).

An infilling crack initiated at one of the interfaces of the fractured layer will propagate to the other interface of the fractured layer. Hackles and rib marks on the infilling fracture surfaces will be similar to the pattern shown in Fig. 13(c).

In the hypothetical diagrams in Fig. 13, the propagation of infilling cracks is considered only in the vertical direction. The results are limited by the two-dimensional nature of the modeling work in this paper. Because of this restriction, we cannot consider infilling processes by lateral fracture propagation. However, the results should conceptually be valid surrounding the origin in a segment of the fractured surface of width approximately equal to the thickness of the fractured layer. In this region, the crack does not propagate predominantly in the horizontal direction, but rather radiates away from the origin as shown by the hackles in Fig. 12.

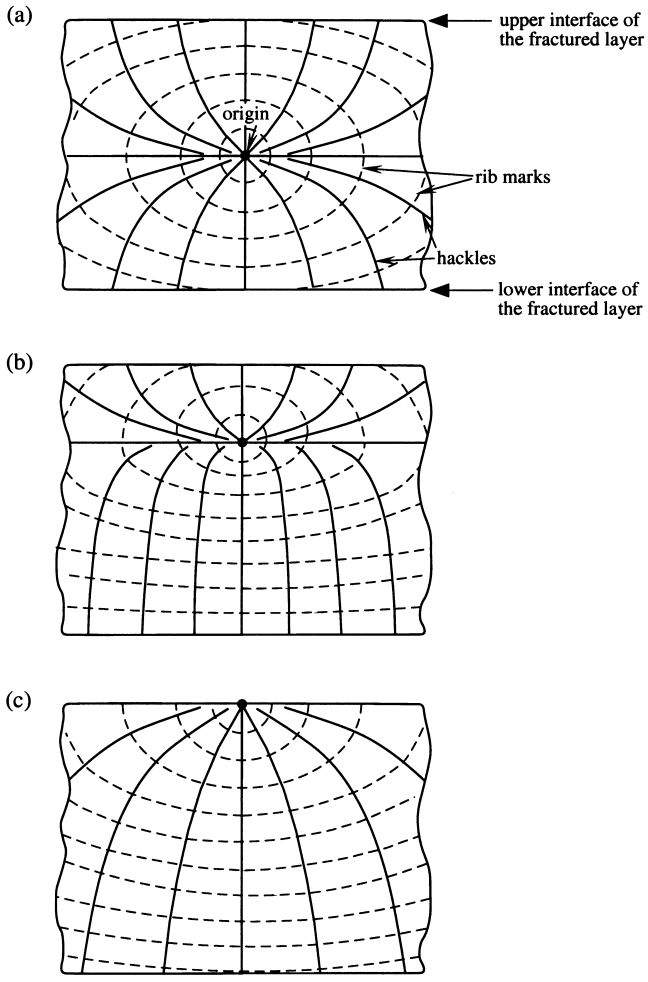


Fig. 13. Cartoon diagram showing the hypothetical surface patterns of infilling fractures initiated from origins: (a) at the middle of the fractured layer; (b) at the upper half of the fractured layer; and (c) at the upper interface of the fractured layer. All the fractures showing here propagate vertically. See text for the details.

### 3.5. Terminated cracks within the fractured layer

*Terminated cracks* between adjacent fractures include that infilling cracks stopped before they cut through the fractured layer, and flaws or cracks that did not grow under the remote extension. The occurrence of terminated cracks depends on the location of the crack, the ratio of fracture spacing to layer thickness, the applied strain and the fracture toughness of the material. The numerical results imply that three types of terminated cracks may be found between adjacent fractures. The first type consists of cracks in the middle of the fractured layer and between fractures with a spacing to layer thickness ratio less than the critical ratio defined by the stress transition. The heights of these cracks are less than the critical crack size (Fig. 7). Because the stress intensity factors of these cracks are negative (Fig. 6) regardless of the applied average strain and the fracture toughness of the material, these cracks cannot have any further growth.

Terminated cracks of the second type develop from flaws close to the upper or lower interface of the fractured layer when the ratio of spacing to layer thickness of the fractures is less than the critical value for complete infilling (Fig. 10). In this case, the stress intensity

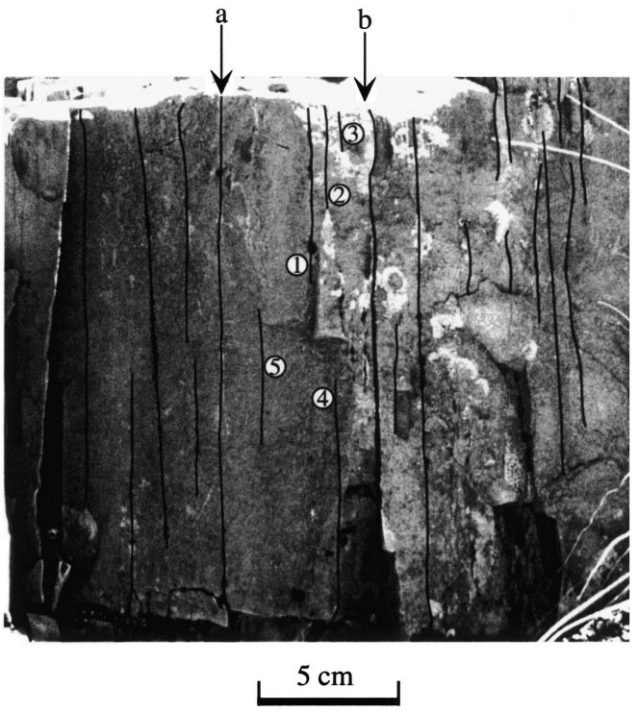


Fig. 14. Through cutting joints and terminated cracks in a limestone layer from the Carmel Formation, Chimney Rock, Utah. Some of the features are line traced.

factor of a growing infilling crack changes from positive to negative before the crack reaches the height of the fractures (Fig. 8). The heights of the cracks depend on the average strain and the fracture toughness of the material. The maximum height of these fractures is a function of the spacing to layer thickness ratio of the fractures (Figs. 9 and 10).

These two types of terminated cracks are commonly found in a limestone layer in the Carmel Formation of Chimney Rock, Utah. The layer is quite homogeneous in terms of lacking fossils and bed structures, and is cryptocrystalline (Taylor, 1981). In Fig. 14, the two joints (a and b) indicated by the arrows cut through the fractured layer. Their spacing to layer thickness ratio is about 0.35, which is less than the critical value for complete infilling. Between the two joints several terminated cracks are found. Cracks 1, 2 and 3 are located with their upper tips at the upper interface of the fractured layer. Crack 4 is located with its lower tip at the lower interface of the layer. Based on the modeling results, we conclude that these cracks are terminated infilling cracks because the spacing to layer thickness ratio of joints a and b is less than the critical value for complete infilling. It is also noted that there is another crack between joints a and b labeled as crack 5. This crack is approximately centered at the middle of the fractured layer. Given the spacing to layer thickness ratio of joints a and b, we know from Fig. 7 that the normalized critical flaw size is about 0.8. The normalized height of crack 5 is about 0.25, which is less than the critical flaw size, i.e. $K_I < 0$. This accounts for why crack 5 did not grow to the interfaces to form a through fracture.

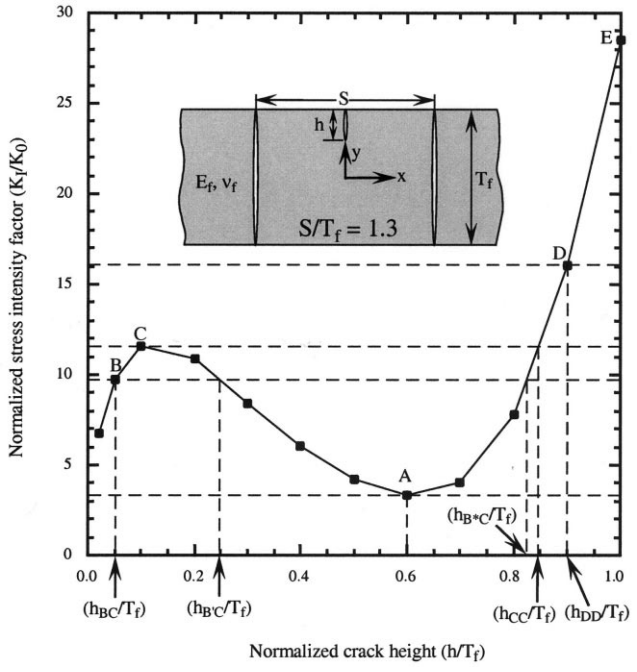


Fig. 15. The normalized stress intensity factor of the lower tip of a crack with its upper tip at the upper interface of the fractured layer as a function of crack height. Refer to the text for the details of the propagation behavior of the crack.

The third type of terminated cracks include those developed from flaws close to the interfaces and the flaws themselves between fractures with spacing to layer thickness ratios greater than the critical ratio for complete infilling and less than the critical ratio for unstable growth. Their existence depends upon the relative magnitudes of the fracture toughness of the material and the stress intensity factor, i.e. the resistance and the driving force.

To understand terminated cracks of this type more clearly, we show an example in Fig. 15. For the model configuration given in the figure, if the fracture toughness of the material is greater than the stress intensity factor at point E, the crack cannot grow, no matter what its height. Therefore, the existing crack is a terminated crack. If the fracture toughness of the material is less than the stress intensity factor at point E and greater than that at point C, the crack is a terminated crack if its height is less than a critical size. This critical height is between $h_{CC}$ and $T_f$, and is determined by the specific value of the fracture toughness of the material. For example, if the fracture toughness is equal to the stress intensity factor at point D, the crack cannot grow if its height is less than $h_{DD}$.

The situation becomes more complicated when the fracture toughness is greater than the stress intensity factor at point A, but less than the stress intensity factor at point C. For example, if the fracture toughness is equal to the stress intensity factor at point B, the crack cannot grow if its height is less than $h_{B*C}$ or greater than $h_{B'C}$ and less than $h_{B*C}$. If the height of the crack is between $h_{BC}$ and $h_{B'C}$, it will grow to reach the height of $h_{B'C}$, then stop and become a terminated crack. If the fracture toughness of the material is less than the stress intensity factor at point A, the crack will propagate to the lower interface once it starts to propagate.

## 4. Conclusions

For a layered system with fracture spacing to layer thickness ratio less than the critical value, the initiation points of infilling fractures are more likely to be found near the interfaces than in the middle of the fractured layer. In order for a crack in the middle of the fractured layer to propagate, its height has to be greater than a critical size, which decreases with increasing ratio of fracture spacing to layer thickness. At the critical spacing to layer thickness ratio, the critical size reduces to zero.

An infilling fracture, developed from a crack with

one of its tips located at the interface, can cut through the fractured layer (complete infilling) only if the fracture spacing to layer thickness ratio is greater than the critical value for complete infilling. Otherwise, the infilling fracture can only partially cut the fractured layer (partial infilling). The minimum spacing to layer thickness ratio is half of the critical spacing to layer thickness ratio for complete infilling. For models with the same elastic constants for the fractured layer and the neighboring layers, this critical value for complete infilling is 0.546, and the minimum fracture spacing to layer thickness ratio is 0.273. Mechanisms other than pure extension (i.e. internal fluid pressure) apparently are required in order to explain the formation of fractures with spacing to layer thickness ratios less than half the critical ratio for complete infilling.

The propagation of a crack in the middle of the fractured layer is unstable. The propagation behavior of a crack with one of its tips at the interface is more complicated: it is unstable when the fracture spacing to layer thickness ratio is greater than a critical value $(S/T_f)^u_{cr}$; and first unstable, then stable, and then unstable again when the spacing ratio is less than $(S/T_f)^u_{cr}$. For models with the same elastic constants for the fractured layer and the neighboring layers, the ratio $(S/T_f)^u_{cr}$ is 1.53. This implies that fracture propagation in infilling processes that produce joints of spacing to layer thickness ratios in Range III is first unstable, then stable, and then unstable again.

## Acknowledgements

This research is supported by the Stanford Rock Fracture Project and the National Science Foundation grant No. EAR-9805324. We thank Atilla Aydin, Huajian Gao, Michael Gross, Gary Mavko, and Yongjun Yue for their valuable discussion and suggestions. Reviews by Terry Engelder, James Evans and an anonymous reviewer greatly improved the quality of this paper.

## References

Anderson, T.L., 1995. Fracture Mechanics. CRC Press, Boca Raton.

Ashby, M.F., Hallam, S.D., 1986. The failure of brittle solids containing small cracks under compressive stress states. Acta Metallurgica 34, 497–510.

Bai, T., Pollard, D.D., 2000. Fracture spacing in layer rocks: a new explanation. Journal of Structural Geology 22, 43–57.

Bai, T., Pollard, D.D., Gross, M.R., 2000. Mechanical prediction of fracture aperture in layered rocks. Journal of Geophysical Research 105, 707–721.

Bankwitz, P., Bankwitz, E., 1995. Fractographic features on joints of KTB drill cores (Bavaria, Germany). In: Ameen, M.S. (Ed.), Fractography: fracture topography as a tool in fracture mechanics and stress analysis, Geological Society Special Publication, No. 92, pp. 39–58.

Becker, A., Gross, M.R., 1996. Mechanism for joint saturation in mechanically layered rocks: an example from southern Israel. Tectonophysics 257, 223–237.

Bessinger, B., Cook, N.G.W., 1995. Observations from Vancouver Island, British Columbia, that may indicate compression-driven mode I fracturing occurs on the geologic scale. Proceedings of the 35th U.S. Symposium on Rock Mechanics 35, 703–710.

Bittencourt, T.N., Barry, A., Ingraffea, A.R., 1992. Comparison of mixed-mode stress-intensity factor obtained through displacement correlation, J-integral formulation, and modified crack-closure integral. In: Atluri, S.N., Newman Jr., J.C., Raju, I.S., Epstein, J.S. (Eds.), Fracture Mechanics, Twenty-Second Symposium (volume II), ASTM STP 1131. American Society for Testing and Materials, Philadelphia, pp. 69–82.

Bittencourt, T.N., Wawrzynek, P.A., Ingraffea, A.R., Sousa, J.L., 1996. Quasi-automatic simulation of crack propagation for 2D LEFM problems. Engineering Fracture Mechanics 55, 321–334.

Brace, W.F., Bombolakis, E.G., 1963. A note on brittle crack growth in compression. Journal of Geophysical Research 68, 3709–3713.

Brace, W.F., 1966. Dilatancy in the fracture of crystalline rocks. Journal of Geophysical Research 71, 3939–3953.

DeGraff, J.M., Aydin, A., 1987. Surface morphology of columnar joints and its significance to mechanics and direction of joint growth. Geological Society of America Bulletin 99, 605–617.

DeGraff, J.M., Aydin, A., 1993. Effect of thermal regime on growth increment and spacing of contraction joints in basaltic lava. Journal of Geophysical Research 98, 6411–6430.

Dyskin, A.V., 1993. A-2 model of skin rock burst and its application to rock burst monitoring. In: Szwedzicki, T. (Ed.), Geotechnical Instrumentation and Monitoring in Open Pit and Underground Mining. Proceedings of the Australian Conference. A.A. Balkema, Rotterdam, pp. 133–141.

Eidelman, A., Reches, Z., 1992. Fractured pebbles: a new stress indicator. Geology (Boulder) 20, 307–310.

Engelder, T., 1987. Joint and shear fractures in rock. In: Atkinson, B. (Ed.), Fracture Mechanics of Rock. Academic Press, pp. 27–69.

Fairhurst, C., Cook, N.G.W., 1966. The phenomenon of rock splitting parallel to the direction of maximum compression in the neighborhood of a surface. In: Proceeding of the 1st International Society of Rock Mechanics Congress, Lisbon, pp. 687–692.

Fischer, M.P., Gross, M.R., Engelder, T., Greenfield, R.J., 1995. Finite-element analysis of the stress distribution around a pressurized crack in a layered elastic medium: implications for the spacing of fluid-driven joints in bedded sedimentary rock. Tectonophysics 247, 49–64.

Gallagher Jr., J.J., Friedman, M., Handin, J., Sowers, G.M., 1974. Experimental studies relating to microfracture in sandstone. Tectonophysics 21, 203–247.

Germanovich, L.N., Carter, B.J., Dyskin, A.V., Ingraffea, A.R., Lee, K.K., 1996. Mechanics of 3-D crack growth under compressive loads. In: Hassani, F., Mitri, H.S. (Eds.), Proceedings of the 2nd North American rock mechanics symposium. A.A. Balkema, Rotterdam, pp. 1151–1160.

Gross, M.R., 1993. The origin and spacing of cross joints: examples from Monterey Formation, Santa Barbara Coastline, California. Journal of Structural Geology 15, 737–751.

Gross, M.R., Bahat, D., Becker, A., 1997. Relations between jointing and faulting based on fracture-spacing ratios and fault-slip profiles: A new method to estimate strain in layered rock. Geology 25, 887–890.

Gross, M.R., Engelder, T., 1995. Fracture strain in adjacent units of the Monterey Formation: Scale effects and evidence for uniform

displacement boundary conditions. Journal of Structural Geology 17, 1303–1318.

Gross, M.R., Fischer, M.P., Engelder, T., Greenfield, R.J., 1995. Factors controlling joint spacing in interbedded sedimentary rocks: integrating numerical models with field observations from the Monterey Formation, USA. In: Ameen, M.S. (Ed.), Fractography: fracture topography as a tool in fracture mechanics and stress analysis, Geological Society Special Publication, No. 92, pp. 215–233.

Helgeson, D.E., Aydin, A., 1991. Characteristics of joint propagation across layer interfaces in sedimentary rocks. Journal of Structural Geology 13, 897–911.

Hodgson, R.A., 1961. Regional study of jointing in Comb Ridge–Navajo Mountain area, Arizona and Utah. American Association of Petroleum Geologists Bulletin 45, 1–38.

Horii, H., Nemat-Nasser, S., 1985. Compression-induced microcrack growth in brittle solids: Axial splitting and shear failure. Journal of Geophysical Research 90, 3105–3125.

Huang, Q., Angelier, J., 1989. Fracture spacing and its relation to bed thickness. Geological Magazine 126, 355–362.

Ingraffea, A.R., 1990. Case studies of simulation of fracture in concrete dams. Fracture Mechanics 35, 553–564.

Ishido, T., Nishizawa, O., 1984. Effects of zeta potential on microcrack growth in rock under relatively low uniaxial compression. Journal of Geophysical Research 89, 4153–4159.

Jaeger, J.C., Cook, N.G.W., 1979. Fundamentals of Rock Mechanics, 3rd edition. Chapman and Hall, London.

Kemeny, J., Cook, N.G.W., 1987. Determination of rock fracture parameters from crack models for failure in compression. In: Daemen, J.J.K., Desai, C.S., Glass, C.E., Neuman, S.P. (Eds.), Proceedings of the 28th U.S. Symposium on Rock Mechanics, 28, pp. 367–374.

Kulander, B.R., Barton, C.C., Dean, S.L., 1979. The application of fractography to core and outcrop fracture investigations. US Department of Energy, Morgantown Energy Technology Center, Morgantown, W.Va.

Kulander, B.R., Dean, S.L., Ward, B.J., 1990. Fractured core analysis: Interpretation, lodging, and use of natural and induced fractures in core. In: AAPG Methods in Exploration Series, 8. American Association of Petroleum Geologists, Tulsa, Oklahoma.

Ladeira, F.L., Price, N.J., 1981. Relationship between fracture spacing and bed thickness. Journal of Structural Geology 3, 179–183.

Lawn, B.R., 1993. Fracture of Brittle Solids, 2nd edition. Cambridge University Press, Cambridge, New York.

Linsbauer, H.N., Ingreffea, A.R., Rossmanith, H.P., Wawrzynek, P.A., 1989. Simulation of cracking in large arch dam: Part I. Journal of Structural Engineering 115, 1599–1615.

McQuillan, H., 1973. Small-scale fracture density in Asmari Formation of southwest Iran and its relation to bed thickness and structural setting. American Association of Petroleum Geologists Bulletin 57, 2367–2385.

Narr, W., Lerche, I., 1984. A method for estimating subsurface fracture density in core. American Association of Petroleum Geologists Bulletin 66, 637–648.

Narr, N., Suppe, J., 1991. Joint spacing in sedimentary rocks. Journal of Structural Geology 13, 1037–1048.

Nemat-Nasser, S., Sumi, Y., Keer, L.M., 1980. Unstable growth of tension cracks in brittle solids: stable and unstable bifurcations, snap-through, and imperfection sensitivity. International Journal of Solids and Structures 16, 1017–1035.

Pollard, D.D., Aydin, A., 1988. Progress in understanding jointing over the past century. Geological Society of America Bulletin 100, 1181–1204.

Pollard, D.D., Segall, P., 1987. Theoretical displacements and stresses near fractures in rocks: with applications to faults, joints, veins, dikes and solution surfaces. In: Atkinson, B.K. (Ed.), Fracture Mechanics of Rock. Academic Press, London, pp. 277–349.

Price, N.J., 1966. Fault and Joint Development in Brittle and Semi-Brittle Rocks. Pergamon Press, Oxford.

Price, N.J., Cosgrove, J.W., 1990. Analysis of Geological Structures. Cambridge University Press, Cambridge.

Raju, I.S., 1987. Calculation of strain-energy release rates with higher order and singular elements. Engineering Fracture Mechanics 28, 251–274.

Renshaw, C.E., Harvey, C.F., 1994. Propagation velocity of a natural hydraulic fracture in a poroelastic medium. Journal of Geophysical Research 99, 21659–21677.

Rybicki, E.F., Kanninen, M.F., 1977. A finite element calculation of stress intensity factors by modified crack closure integral. Engineering Fracture Mechanics 9, 931–938.

Taylor, D.W., 1981. Carbonate petrology and depositional environments of the limestone member of the Carmel Formation, near Carmel Junction, Kane County, Utah. Geology Studies 28, 117–133.

Wang, R., Kemeny, J.M., 1994. A new empirical failure criterion for rock under polyaxial compressive stresses. Proceedings of the 35th U.S. Symposium Rock Mechanics 35, 453–458.

Wawrzynek, P.A., Ingraffea, A.R., 1987. Interactive finite element analysis of fracture processes: An integrated approach. Theoretical and Applied Fracture Mechanics 8, 137–150.

Weinberger, R., 1999. Initiation and growth of cracks during desiccation of stratified muddy sediments. Journal of Structural Geology 21, 379–386.

Woodworth, J.B., 1897. On the fracture system of joints, with remarks on certain great fractures. Proceedings of the Boston Society of Natural History 27, 163–183.

Wu, H., Pollard, D.D., 1995. An experimental study of the relationship between joint spacing and layer thickness. Journal of Structural Geology 17, 887–905.